Author's Accepted Manuscript

Bubble transport mechanism: Indications for a gas bubble-mediated inoculation of benthic methanotrophs into the water column

Oliver Schmale, Ira Leifer, Jens Schneider v. Deimling, Christian Stolle, Stefan Krause, Katrin Kießlich, Andreas Frahm, Tina Treude

Cite this article as: Oliver Schmale, Ira Leifer, Jens Schneider v. Deimling, Christian Stolle, Stefan Krause, Katrin Kießlich, Andreas Frahm and Tina Treude, Bubble transport mechanism: Indications for a gas bubble-mediated inoculation of benthic methanotrophs into the water column, *Continental Shelf Research*, http://dx.doi.org/10.1016/j.csr.2015.04.022

This is a PDF file of an unedited manuscript that has been accepted for publication. As a service to our customers we are providing this early version of the manuscript. The manuscript will undergo copyediting, typesetting, and review of the resulting galley proof before it is published in its final citable form. Please note that during the production process errors may be discovered which could affect the content, and all legal disclaimers that apply to the journal pertain.

Bubble Transport Mechanism: Indications for a gas bubble-mediated inoculation of benthic methanotrophs into the water column

Oliver Schmale[1*], Ira Leifer[2,3], Jens Schneider v. Deimling[4], Christian Stolle[1], Stefan Krause[4], Katrin Kießlich[1], Andreas Frahm[1] and Tina Treude[4,5]

[1]   Leibniz Institute for Baltic Sea Research Warnemünde (IOW), Seestrasse 15, D-18119 Rostock, Germany

[2]   University of California, Santa Barbara (UCSB), Santa Barbara, CA 93106, USA

[3]   Bubbleology Research International, Solvang, CA 93463, USA

[4]   GEOMAR Helmholtz Centre for Ocean Research Kiel, Wischhofstrasse 1-3, D-24148 Kiel, Germany

[5]   Present address: University of California, Los Angeles, Department of Earth, Planetary & Space Sciences and Atmospheric & Oceanic Sciences, Los Angeles, CA 90095, USA

*   Correspondence to:

    Oliver Schmale

    E-mail address: oliver.schmale@io-warnemuende.de

    Phone number: +49 3815197305

    Postal address: Seestrasse 15, D-18119   Rostock, Germany

Abstract

The importance of methanotrophic microorganisms in the sediment and water column for balancing marine methane budgets is well accepted. However, whether methanotrophic populations are distinct for benthic and pelagic environments or are the result of exchange processes between the two, remains an area of active research. We conducted a field pilot

study at the Rostocker Seep site (Coal Oil Point seep field, offshore California, USA) to test the hypothesis that bubble-mediated transport of methane-oxidizing microorganisms from the sediment into the water column is quantifiable. Measurements included dissolved methane concentration and showed a strong influence of methane seepage on the water-column methane distribution with strongly elevated sea surface concentrations with respect to atmospheric equilibrium (saturation ratio ~17,000%).

Using Catalyzed Reporter Deposition Fluorescence In Situ Hybridization (CARD FISH) analysis, aerobic methane oxidizing bacteria (MOB) were detected in the sediment and the water column, whereas anaerobic methanotrophs (ANME-2) were detected exclusively in the sediment. Critical data for testing the hypothesis were collected using a novel bubble catcher that trapped naturally emanating seep gas bubbles and any attached particles approximately 15 cm above the seafloor. Bubble catcher experiments were carried out directly above a natural bubble seep vent and at a nearby reference site, for which an "engineered" nitrogen bubble vent without sediment contact was created. Our experiments indicate the existence of a "Bubble Transport Mechanism", which transports MOB from the sediment into the water column. In contrast, ANME-2 were not detected in the bubble catcher. The Bubble Transport Mechanism could have important implications for the connectivity between benthic and pelagic methanotrophic communities at methane seep sites.

Keywords: gas vent, methane, bentho-pelagic bubble transport, methanotrophs

1. Introduction

After water vapor and carbon dioxide (CO_2), methane is the most relevant greenhouse gas on earth, contributing about 20% to radiative forcing by well-mixed greenhouse gases on a century timescale (IPCC, 2013). Significant natural marine methane sources are mud volcanoes (Etiope and Klusman, 2002), hydrothermal systems (Schmale et al., 2012b), and

2

cold hydrocarbon seeps (Judd and Hovland, 2007). Due to global warming, flooded permafrost (Shakhova et al., 2010) and submarine Arctic gas hydrates (Berndt et al., 2014; Westbrook et al., 2009) are currently under debate as additional drivers for increasing marine methane emissions to the atmosphere.

Due to their high organic matter content, continental slope and marginal sea sediments have huge methane generation potential by biogenic or thermogenic processes (Judd and Hovland, 2007; Reeburgh, 2007). In areas where methane is present in sediment pore fluids or in the water column, it serves as an important energy and carbon source for a complex microbial community (Knittel and Boetius, 2009; Valentine, 2011). Depending on the availability of methane and either oxygen or sulfate, microbial methane oxidation in the marine environment is conducted by aerobic methane-oxidizing bacteria (MOB) and anaerobic methanotrophic archaea (ANME), respectively. Although ANME activity is more relevant in the sediment, MOB represent the dominant microbial methane sink in the water column. MOB can be subdivided into the three main groups, Type I, II and X (Hanson and Hanson, 1996). There are three phylogenetically distinct groups of ANME (ANME-1, 2, and 3), which are commonly associated with sulfate-reducing bacteria (Knittel et al., 2005). This so called "benthic methane filter" (Sommer et al., 2006) is very efficient and removes a major fraction of upward-migrating, dissolved methane in sediments by converting it into carbonates (Peckmann et al., 2001) and biomass (Nauhaus et al., 2007). In addition to sediment processes, the pelagic methane filter is dominated by MOB that decrease dissolved water column methane before it can enter the atmosphere (Reeburgh, 2007). In the water column, time-scales of microbial methane degradation below the wave-mixed layer are relatively short compared to ventilation to the atmosphere, preventing contribution from deep methane to atmospheric methane budgets (Rehder et al., 1999). However, methane bubbles largely bypass the benthic and pelagic microbial filter, enabling highly efficient transport of methane from the sediment towards the sea surface. Dissolution of bubbles rising from the seabed elevates

3

methane concentrations in the overlying water column (McGinnis et al., 2006; Schmale et al., 2010). The vertical distribution of such dissolved methane from gas plumes and hence the potential for atmospheric impact depends on (a) water depth, (b) initial bubble size and gas fraction therein, (c) bubble dissolution kinetics, (d) local oceanographic conditions such as currents and density stratification (Leifer and Patro, 2002; Schmale et al., 2010), and (e) microbial methane oxidation (Valentine et al., 2001). Recent studies in the water column surrounding hydrocarbon seeps indicated an elevated abundance of methanotrophic microorganism in the near field of gas bubble plumes (Schubert et al., 2006). The enhanced methane concentration in the seep-affected water column stimulates the activity of methane oxidizers (Valentine et al., 2001) and might lead to a rise in the abundance of methane-oxidizing microbes in the aging plume water as was shown by Crespo-Medina et al. (2014) in the Deepwater Horizon plume and by de Angelis et al. (1993) in an aged hydrothermal plume.

Laboratory (Zhou and Mopper, 1998), modeling (Sadhal and Johnson, 1983), and field studies (Leifer and Clark, 2002) show that bubbles vertically transport surface-active substances (surfactants). Surfactants are compounds with hydrophobic and hydrophilic characteristics, which readily attach to gas/water interfaces (Schaefer et al., 1998; Wan and Wilson, 1994). To this group of substances belong colloidal, surface active particles which can consist of mineral particles (clay), organic macromolecules (proteins, lipids, and hydrocarbons), and even bacteria and viruses (Wan and Wilson, 1994).

Laboratory studies have shown that the accumulation of microorganisms on bubble surfaces facilitates their transport through a sandy matrix (Powelson and Mills, 1998; Wan et al., 1994). In contrast to studies regarding the transport of colloids on gas/water interfaces within groundwater environments (e.g., Powelson and Mills, 1998; Wan and Wilson, 1994; Wan et al., 1994), the relevance of this transport mechanism for the marine environment is discussed only rudimentarily in the literature (Leifer and Judd, 2002; Schubert et al., 2006). The accumulation of particles at the sea surface/atmosphere interface and the controlling

4

mechanisms have long been the subject of different scientific investigations (e.g., Cunliffe et al., 2013; and references therein). In this interface, wind-driven surface-waves break and form bubble clouds. This well-studied mechanism sparges particles and surface active substances in the upper water column and transports them to the sea-surface microlayer (Bezdek and Carlucci, 1972; Wallace and Duce, 1978). This transport mechanism is hypothesized to influence microorganism abundance and microbial community diversity in the sea-surface microlayer (Cunliffe et al., 2013). Laboratory studies also show that bacterial enrichment at the sea-surface (the so-called bacterioneuston) affects air-sea gas exchange (Upstill-Goddard et al., 2003).

Studies at the sediment/water interface showed that resuspension (Shimeta et al., 2002) and submarine fluid discharge (Campbell et al., 2013) can transport microorganisms from the sediment into the water column and that these transport mechanisms have implications on the microbial community structure within the water column. Here, we hypothesize that a bubble-mediated transport mechanisms between the benthic and pelagic habitats represents an additional exchange process. More specifically, for an environment influenced by gas seepage, we hypothesize that gas bubbles transport methanotrophic microorganisms from the sediment into the water column, a process we termed the "Bubble Transport Mechanism". This hypothesized mechanism would influence the water column methanotrophic community, thereby indirectly providing feedback mechanisms for dissolved methane concentrations in the water column with the potential to impact the sea/atmosphere methane flux. To test our bubble transport hypothesis we conducted a pilot field study at a natural gas bubble seepage area (informally named Rostocker Seep) in the Coal Oil Point seep field, offshore Southern California, USA. Key to this pilot study was the development of a bubble collection device (bubble catcher) that collected gas bubbles after they emerged from the seafloor together with any attached surfactant particles.

2. Material and Methods

2.1 Study site

The Santa Barbara basin (California, USA) contains one of the world's largest and best investigated hydrocarbon seep fields, the Coal Oil Point seep field (Allen et al., 1970; Clark et al., 2003; Hornafius et al., 1999; Fig. 1). The seep field is located in water depths between a few meters to 80 m, extending from near the beach to 3 km offshore (Hornafius et al., 1999; Leifer et al., 2010). Seepage is concentrated above the Coal Oil Point and South Ellwood Anticlines, which harbors Miocene age oil in the Monterey Formation (Fischer, 1977).

A wide diversity of seepage has been documented in the Coal Oil Point seep field from sporadic single bubble vents releasing gentle bubble emanations to intense high-flow vents that span a broad range of bubble sizes, although generally radius r > 1000 μm (Leifer, 2010). Mean seep gas composition is 87.5% methane, 5.1% ethane, 3.1% propane and 1.3% carbon dioxide along with trace gases of heavier hydrocarbons and hydrogen sulfide (Clark et al., 2000). Some emission sites are constant, others eruptive. A further dimension of complexity is the oiliness of most vents, leading to persistent and extensive sea surface oil slicks (Leifer et al., 2006).

Using biomolecular methods and biogeochemical techniques, the process of microbial anaerobic and aerobic CH_4 oxidation has been identified clearly in sediments and in the overlying water column of the Coal Oil Point seep field (e.g., Kinnaman et al., 2010; Mau et al., 2012; Treude and Ziebis, 2010). Seep gas composition varies between different regions of the Coal Oil Point seep field. At the Brian Seep site (10 m water depth, 34° 24.109' N; 119° 49.917' W) captured gas consisted of 91% methane, 7% CO_2, 1% ethane, and 0.2% propane (Kinnaman et al., 2010).

Field measurements were made between 15 and 17 February 2012 at the Rostocker Seep site (34° 24.230' N; 119° 50.438' W), which is located northeast of Campus Point and ~30 m northeast of Brian Seep in 10 m water depth (Fig. 1). The site is situated slightly north of the

6

Coal Oil Point Anticline, which strikes approximately east-west through the campus point (Fig. 1; Leifer et al., 2010). Rostocker Seep releases non-oily gas bubbles from primarily sandy sediments. This sediment type is distinct from most other deeper seep sites in the Coal Oil Point seep field, whose sediments are comprised of a mixture of sand and tar. Marine conditions were ideal for sampling, with wave heights of less than 30 cm and calm winds during the study. However, winds and waves during previous days were significant and led to limited water visibility of approximately 0.5-1 m during the study.

2.2   Bubble catching experiment

The key tool developed for this study was a bubble catcher (Fig. 2), whose design was different from previous instruments that have been used to collect gas bubbles for gas composition analysis (Huttunen et al., 2001; Pape et al., 2010). The main difference of this adapted catcher is the sample cylinder, which is pre-filled with sterile-filtered artificial seawater. This setup allows after recovery the collection of microorganisms that were transported into the bubble catcher sample cylinder over the runtime of the experiment.

The bubble catcher was constructed to collect gas bubbles close to the sediment-water interface, i.e., approximately 15 cm above the gas vent, which is the distance between seafloor and the inlet of the stop-cock 2, Fig. 2), and to transfer the bubbles together with attached surface-active substances (surfactants) into an acrylic glass sample cylinder (Fig. 3A). The cylinder was filled with sterile-filtered artificial seawater (filter size 0.2 μm, salinity 35, total volume of the bubble catcher sample cylinder 8.8 L) prior to deployment. The transported surfactants (including bacterial cells) then accumulated in the bubble catcher at the water/gas interface upon bubble bursting (Fig. 3B).

The bubble catcher was lowered to the seafloor using a davit, and positioned above a gas vent by scuba divers. After deployment, the divers waited for about 2 minutes before opening the sample cylinder using stop-cock 2 (Fig. 2), to allow the settlement of particles

resuspended from the seafloor. The scuba divers and the bubble catcher were monitored continuously onboard during the experiments with a video system attached to the frame of the bubble catcher.

In total two studies were conducted. The first study was dedicated to catch gas bubbles and attached microbes from a natural gas vent (hereafter termed "BC vent"; Fig. 3A). A second study, conducted about 1 hour after the "BC vent" experiment at the same location, was directed to obtain a water-column background value of microbes collected and transported by bubbles that had not been in contact with sediment (hereafter termed "BC blank"). The setup of the "BC blank" experiments was developed to establish experimental condition similar to the "BC vent" experiment (Fig. 2). However, different to the "BC vent" experiment, the bubble catcher was positioned at about 50 cm distance from the gas vent and bubbles were created from a pressurized nitrogen tank through a 1/8″ diameter tube whose outlet was placed between the seafloor and the funnel of the bubble catcher (Fig. 2). Pressure was calibrated in the laboratory and monitored during sampling to provide an artificial bubble stream that appeared qualitatively similar to the nearby natural vents. The experimental runtimes and gas volumes collected with the bubble catcher were quite similar (4.15 L gas in 95 min for "BC vent", 4.00 L gas in 75 min for "BC blank"). The longer runtime of the "BC vent" experiment can be explained by the transient bubble emission from the "BC vent" site that could not be considered in the "BC blank" experiment (see 3.1). On board the vessel, water samples from these two experiments were subsampled into sterile bottles as described below and the bubble catcher was rinsed carefully with sterile-filtered artificial seawater (see above) to collect all microbial cells out of the bubble catcher for quantitative analyses.

2.3   Gas bubble measurements

The gas bubble measurements were conducted about 2 hours after the "BC vent" experiment at the same gas vent. For bubble size and gas flux analyses we used the bubble

8

measurement system described in detail by Leifer (2010). The bubble measurement system consisted of a video camera (Super Seacam 6500, Deepsea Power and Light, San Diego, CA), back illumination facilitated by underwater LED lights, an aluminum framework, and blocking components that constrained rising bubbles to a known distance from the camera to minimize parallax errors. Scuba divers positioned the bubble measurement system on the seafloor, which was cabled to the boat for recording, and camera control by a custom video controller. Video analysis to derive the bubble size distribution was carried out according to (Leifer, 2010). Parallax size uncertainty was approximately ±5% (Leifer et al., 2003).

2.4   Water column and sediment sampling

Different types of water-column samples were taken directly above the bubble catcher sampling site. The sea-surface microlayer was sampled using a glass plate sampling technique with a framed wiper (Stolle et al., 2009). This technique collects water samples and particles therein of up to a 50 µm thick film of the sea-surface microlayer. Approximately 100 single glass plate dips were needed to yield a total volume of 1 L. Mid-water column samples were collected with a 2-L sample bottle (LIMNOS, Finland) that was deployed manually on a rope to specific water depths. The bottle was closed with a drop weight at the respective depths during each haul. Divers collected near-seabed water samples using an empty 1-L PET bottle that was opened and filled a few centimeters above the sediment-water interface.

After water column work was finished, sediment samples were recovered close to "BC vent" spot (distance 10 cm) using steel plates (dimension 20 x 30 cm) that were pushed into the sediment by scuba divers. The plates were prepared with drilled holes (closed with plastic tape, 18 vertical holes, hole distance 1 cm) to allow underwater sediment sampling with plastic syringes (volume 5 ml). From the far side of the gas vent spot, the scuba divers removed the sediment, opened the plate holes, and sampled the sediment with the syringes

9

horizontally. Sediments to depths of up to only 12 cm were sampled because the sandy sediment was underlain by a gravel bed.

After collection in the field, samples for gas analyses and molecular biological studies were transferred directly into sample-specific containers onboard the research vessel (see details below).

2.5   Methane analyses

A 600 ml subsample from each water-column sample bottle was transferred into pre-evacuated 1100 ml glass bottles. The dissolved methane was extracted by the use of a vacuum degassing line and a subsample of the gas was transferred into 10 ml pre-evacuated crimp-top glass vials containing 4 ml of supersaturated salt solution (Schmale et al., 2012a). The vials were sealed with a butyl rubber septum and stored "upside-down" to prevent gas exchange with the atmosphere until analysis in the home laboratory. The methane concentration was determined using a gas chromatograph (Trace GC, Thermo Fisher Scientific Inc.) equipped with a flame ionization detector (average precision of $\pm 3\%$).

For respective determinations in sediments, a 4-ml subsample of each sediment sample was transferred into 20-ml crimp-top glass vials containing 10 ml of 2.5% NaOH solution to stop microbial activity. Vials were sealed with a butyl rubber septum and stored inverted until analyzed in the laboratory. The methane concentration were determined as described for the water samples above.

2.6   Quantification of MOB and ANME

From each sediment sample, 0.5 cm^3 were fixed following the protocol of Treude and Ziebis (2010). In the home laboratory, fixed samples were diluted (1:3000) with phosphate-buffered saline (PBS) and treated by mild sonication for 25 s with a Sonotrode probe (Bandelin electronic, Type UW200) at an amplitude of 20% (40W), cycle at 15% (0.15 s). An

aliquot of 1000 µl was filtered on 0.2-µm GTTP polycarbonate filters (Millipore). The filters were embedded in low-gelling-point agarose and frozen at -20°C until further processing.

Water samples (including bubble catcher samples) were collected in 100-ml glass bottles. After fixation with formaldehyde (2% , max. 30 min.), a 50-ml sample from the water column and 100-ml sample from the "BC vent" and "BC blank" experiments were filtered on Nucleopore filters (Whatman, pore size 0.2 µm). Filters were stored at -20°C until further processing.

For the quantification of active MOB and ANME, Catalysed Reporter Deposition Fluorescence In Situ Hybdridization (CARD-FISH) followed by tyramide signal amplification was performed with filters from sediment and water samples according to the protocol of Pernthaler et al. (2002) except for the cell wall permeabilization step. For permeabilization of archaeal cell walls, agarose-embedded filters were incubated in PBS (pH 7.6) containing 0.5% (w/v) sodium dodecyl sulfate (SDS) for 10-15 min at room temperature, washed in MilliQ water, and then dehydrated in absolute ethanol. For permeabilization of bacterial cells, agarose-embedded filters were incubated with lysozyme solution (10 mg ml-1) and incubated for 60 min at 37°C. Binding of streptavidin-HRP to biotin-labeled oligonucleotide probes and tyramid signal amplification was realized using the TSA™ Kit #22 with HRP-streptavidin and Alexa Flour® 488 tyramide (Invitrogen, Karlsruhe) according to the manufacturer's instructions. The following probe/probe mixtures for ANME and aerobic MOB were used: (i) ANME 2-538 (Treude et al., 2007) specific for ANME-2 archaea (40% formamide, hybridization temperature of 46°C), (ii) a mixture (1:1:1) of M(α)450 specific for type II methanotrophs (Eller et al., 2001), and M(γ)84 and M(γ)705 (Eller et al., 2001) specific for type I methanotrophs (20% formamide, hybridization temperature of 46°C). ANME-2 probes were selected, because this type of ANME has been detected nearby to the sampling site in a previous study (Treude and Ziebis, 2010). MOB probes were pooled to ensure maximum detection of aerobic methanotrophs. All hybridized filters were counter stained with 4´,6´-

11

diamidino-2-phenylindole (DAPI). Hybridized and DAPI-stained cells were counted with an epifluorescence microscope (x1000, Leitz Aristoplan). The relative standard deviation for DAPI and CARD-FISH analysis obtained by repetitive cell counting on the same filter were below 5% and 12%, respectively.

3. Results

3.1 Bubble size measurements

The determination of bubble sizes distribution for the "BC vent" site was an important basis to calculate the bubble-mediated flux of microorganisms. Herein we present analysis of ~15 minutes imaging of gas ebullition from the "BC vent" site. Bubble emissions were transient, lasting for tens of seconds - far longer than the wave period (~6 sec) - followed by a period of inactivity lasting tens of seconds before re-activating. Scuba divers reported this emission pattern was widespread at Rostocker Seep during fieldwork. The bubble emission rate was ~20 bubbles per second. The bubble size distribution (Fig. 4) had two dominant emission modes centered at r = 2890 and 1810 μm, where r is the equivalent spherical radius. Both sizes were well fit by Gaussian functions (R^2 = 0.98 and 0.92 for the larger, and smaller emission modes, respectively). The larger mode dominated the volume flux, V, which was well described (R^2=0.9952) by a Gaussian function (not shown) with a peak at r = 3040 μm, while the surface area flux for this mode peaked at 3000 μm (R^2=0.9915).

3.2 Methane concentrations

Methane concentration analyses were carried out to obtain information about methane distribution in the sediment and the seep-surrounding water column (Fig. 5 and 6).

The methane sediment vertical concentration profiles displayed a clear trend from elevated concentrations in the deep sediment towards relatively low concentrations at the sediment surface (Fig. 5A). Water–column methane concentrations surrounding Rostocker Seep

showed strong methane enrichment in the lower water column, decreasing towards the sea surface (Fig. 6A). Despite the decrease, surficial water concentrations were elevated strongly with respect to atmospheric equilibrium (saturation ratio ~17,000%) indicating a non-negligible dissolved methane flux into the atmosphere. Background water-column methane profiles upstream of Rostocker Seep (34°24.177' N; 119°50.445' W) were homogeneous throughout the vertical depth profile with concentrations similar to those for Rostocker Seep lower water column with a mean methane concentration of ~2000 nmol L^{-1} (data not shown).

3.3   Abundance of methanotrophs

DAPI and CARD-FISH analyses were performed on water, sediment, and bubble catcher samples to quantify total microbial cell numbers as well as organism type (ANME-2 and MOB) responsible for methane consumption, and to test the existence of bubble-mediated transport of organisms from the sediment to the water column exists (Fig. 7).

Total cell abundance in the sediment (DAPI staining) increased with decreasing sediment depth showing a maximum of 5×10^{10} cells cm^{-3} sediment at ~1 cm below the sediment surface (Fig. 5B). MOB (CARD-FISH) were most abundant in the sediment surface (1.46×10^9 cells cm^{-3}, 2.9% of DAPI stained cells, Fig. 5B). ANME-2 archaea (CARD-FISH) were present only between 1-3 and at 8 cm sediment depths at numbers of between 1 and 5×10^8 cells cm^{-3} (0.1 to 1.7% of DAPI stained cells, Fig. 5B). Total cell numbers in the water column were on average 5 orders of magnitude lower compared to the sediment. The highest cell numbers (10^6 cells cm^{-3}) were found between 1 and 3 m water depth (Fig. 6B). MOB in the bottom water, in intermediate (5 m) water depths, and in the sea surface microlayer surrounding the Rostocker Seep, revealed similar abundances (~10^3 cells cm^{-3}, 0.2 to 0.4% of DAPI stained cells, Fig. 6). In contrast to these results, ANME-2 were not found in the water column.

13

In the BC experiments, MOB cells were found in the "BC vent" (1.23×10^3 ($\pm 7\%$) cells cm^{-3} (0.4% of DAPI stained cells) but not the "BC blank" sample. No ANME-2 cells were detected in either of the two samples. DAPI analysis showed that the abundance of total cells collected during the "BC vent" experiment (3.42×10^5 ($\pm 4\%$) cells cm^{-3}) was about three times higher than the "BC blank" experiment (1.09×10^5 ($\pm 3\%$) cells cm^{-3}).

4. Discussion

In this study, we confirmed the presence of ANME-2 and MOB in Rostocker Seep sediments, which is in accordance with findings by Treude and Ziebis (2010) for the nearby Brian Seep area. In their study the authors suggested that aerobic methane oxidation is active in the sediment surface layer and anaerobic methane oxidation in sediment layers deeper than 5 cm. Anaerobic methane oxidation was confirmed further by the presence of ANME-2 organisms, whose cell abundance was very similar to our study. In the present study, MOB showed a decreasing trend of abundance with depth, while ANME-2 organisms were present only between 1-3 and 8 cm sediment depth forming a distinct layer where anaerobic methane oxidation probably is occurring (Fig. 5B). The presence of MOB within and below the depth of ANME is surprising, because those two groups should be mutually exclusive given their opposite relationship with oxygen: whereas ANME are inactivated permanently by oxygen (Treude et al., 2005b), MOB depend on oxygen for metabolism. As described by Treude and Ziebis (2010) for Brian Seep, gas bubble migration through permeable sediments can drive pore-water convection that discharges sediment pore water into the ocean (Dando et al., 2000; Haeckel et al., 2007). By continuity, discharged sediment fluid must be replaced, driving a water flow into the sediment. Thus, complex pore water circulation may explain some of the unusual distribution of MOB. Alternatively, or in addition, strong winds and water turbulence at the seafloor, directly preceding the field sampling, could have disturbed previously established zonations of methanotrophic groups along with the sediments.

The bubble catcher experiment above the gas vent revealed the transport of MOB from the sediment into the water column in contrast to the blank experiment, which did not. The complete lack of ANME-2 organisms in the bubble catcher was also in good agreement with the water column findings (Fig. 6B). We hypothesize that the strong oxygen sensitivity of ANME organisms (Treude et al., 2005b) may not allow prolonged water-column survival time even if their exposure to oxygen during the runtime of the experiment and recovery of the water samples was relatively short with a maximum of 120 min. Consequently, the applied CARD-FISH technique would have failed to detect dead ANME-2 cells if present, because the targeted RNA quickly degenerates after cell death (Schippers et al., 2005).

Another aspect that might influence the bubble transport of microorganisms is their specific surface activity (Schaefer et al., 1998). If ANME have a poor surface activity, they might detach from bubbles within a few centimeters after exiting the sediment. Leifer and Culling (2010) observed in tank experiments how non-surface active sediment particles were lofted by bubbles just a few centimeters, before falling from the bubble's trailing edge. Lastly, differences in cell size, shape, or density and position in the sediment may impact the bentho-pelagic transport of microorganisms by gas bubbles. Notably, in the upper 1 cm of the sediment the abundance of MOB was one order of magnitude higher compared to ANME-2 (Fig. 5B).

The transport of water column-born microorganisms into the bubble catcher was evident from the "BC blank" experiment, which showed that about one third of the microorganisms were transported into the sample cylinder without having contact with the sediment. As fluid movement at the Bubble Catcher inlet was not monitored (e.g. by tinting the water within the funnel), the advection of microorganisms from fluids discharged from the seep sediment or by advection of bottom water into the bubble catcher sample cylinder cannot be excluded. We are confident, however, that bubble-mediated transport of cells should be far more efficient (because faster) compared to fluid movement. Therefore we conclude that microorganisms

15

found in the "BC blank" sample cylinder mostly were stripped from the water column by the artificial bubble stream. The fact that no MOB were detected in the "BC blank", despite their presence in the water column surrounding the Rostocker Seep area, indicated that MOB-catch from the short water column between the sediment and the bubble catcher (ca. 15 cm) was of minor relevance during the runtime of the experiments, especially given their low abundance in the water column (Fig. 6) compared to the sediment (Fig. 5).

With the following calculations, we estimated the MOB and the total cell transport rate from the sediment into the water column by the Bubble Transport Mechanism at the studied gas vent. A total gas volume of 4.15 ($\pm$1%) L was collected during the "BC vent" experiment. According to our bubble measurements we assume that the total volume bubble flux was represented by bubbles with volumes of 0.12 ($\pm$16%) cm^3 equivalent to r = 3040 ($\pm$5%) µm, derived from the peak of the volume flux function, resulting in approximately 35,800 ($\pm$17%) bubbles trapped during the "BC vent" experiment. The water sample volume of the "BC vent" experiment was 4.65 ($\pm$1%) L (i.e. water volume that was left in the bubble catcher after the experiment). Based on the concentration of MOB in the "BC vent" water sample (1.23×10^3 ($\pm$7%) MOB cm^{-3}), we estimated that 160 ($\pm$25%) MOB cells were transported per bubble from the sediment into the water. Using our DAPI cell counts from the "BC vent" experiment (3.42×10^5 ($\pm$4%) cells cm^{-3}), which were corrected by the counts of DAPI cells stripped from the water column (1.09×10^5 ($\pm$3%) cells cm^{-3}, "BC blank") and applying the same approach as used in the calculation above, we calculated a bubble transport rate of 30,000 ($\pm$25%) total cells per bubble. The experimental runtime was 95 min, leading to a transport rate of 60×10^3 ($\pm$25%) MOB cells min^{-1} and 11×10^6 ($\pm$25%) total cells min^{-1}. Given a continuous gas release from numerous vents at the Rostocker Seep site and a water column cell abundance between 10^3 and 10^6 cells cm^{-3} we propose that these bubble transport rates are sufficient to alter the pelagic microbial community composition.

However, independent from the existence of such Bubble Transport Mechanism, it should be kept in mind that our pilot study provides no specific information on the survival rate of benthic MOB in the water column. Molecular studies of benthic and pelagic MOB diversity at seeps along the California continental margin indicated rather distinct communities (Tavormina et al., 2008), suggesting that benthic MOB transported by the Bubble Transport Mechanism may not necessarily survive or remain active in the water column over extended time periods.

5. Conclusion

Our pilot field study on a shallow cold seep site with bubble emissions indicated the existence of a bubble-mediated mechanism that transports microorganisms (including methanotrophic bacteria) from the benthic into the pelagic environment. Assuming that the benthic MOB remain active after their transport into the water column, we hypothesize that this Bubble Transport Mechanism contributes to the pelagic methane sink by continuously inoculating the water column with methane-oxidizing microorganisms, adding to the local pelagic MOB population.

Our study was, however, insufficient to evaluate the relevance of the Bubble Transport Mechanism in relation to the abundance of pelagic methanotrophs or other microorganisms in the vicinity of a seep area. Thus, further studies are required to (1) obtain a statistically robust dataset, (2) to parameterize the sediment-water transport efficiency, (3) compare the benthic and pelagic methanotrophic communities on a phylogenetic level, and (4) test the ability of the benthic microorganisms to adapt to the water column environmental conditions. Moreover, the density and distribution of gas vents, the current strength, and the abundance of MOB in the upstream water are important factors that need elucidation to allow a budget approach assessment of the impact of the transported methanotrophic bacteria on the pelagic methane sink.

Acknowledgements

References

Allen, A. A., R. S. Schlueter, and P. G. Mikolaj, 1970. Natural Oil Seepage at Coal Oil Point, Santa Barbara, California, Science 170: 974-977.

Berndt, C., et al., 2014. Temporal Constraints on Hydrate-Controlled Methane Seepage off Svalbard, Science 343: 284-287, doi:10.1126/science.1246298.

Bezdek, H. F., and A. F. Carlucci, 1972. Surface concentration of marine bacteria, Limnol. Oceanogr. 17: 566-569.

Campbell, B. J., S. W. Polson, L. Zeigler Allen, S. J. Williamson, C. K. Lee, K. E. Wommack, and S. C. Cary, 2013. Diffuse flow environments within basalt- and sediment-based hydrothermal vent ecosystems harbor specialized microbial communities, Frontiers in Microbiology 4, doi:10.3389/fmicb.2013.00182.

Clark, J., L. Washburn, J. S. Hornafius, and B. P. Luyendyk 2000. Dissolved hydrocarbon flux from natural marine seeps to the southern California Bight, J. Geophys. Res. 105: 11509-11522.

Clark, J. F., I. Leifer, L. Washburn, and B. P. Luyendyk, 2003. Compositional changes in natural gas bubble plumes: obsercations from the Coal Oil Point marine hydrocarbon seep field, Geo-Mar. Lett. 23: 187-193.

Crespo-Medina, M., et al., 2014. The rise and fall of methanotrophy following a deepwater oil-well blowout, Nature Geosci 7: 423-427, doi:10.1038/ngeo2156 http://www.nature.com/ngeo/journal/v7/n6/abs/ngeo2156.html#supplementary-information.

Cunliffe, M., A. Engel, S. Frka, B. Gašparović, C. Guitart, J. C. Murrell, M. Salter, C. Stolle, R. Upstill-Goddard, and O. Wurl, 2013. Sea surface microlayers: A unified physicochemical and biological perspective of the air–ocean interface, Prog. Oceanogr. 109: 104-116, doi:http://dx.doi.org/10.1016/j.pocean.2012.08.004.

Dando, P. R., et al., 2000. Hydrothermal studies in the aegean sea, Physics and Chemistry of the Earth, Part B: Hydrology, Oceans and Atmosphere 25: 1-8, doi:http://dx.doi.org/10.1016/S1464-1909(99)00112-4.

de Angelis, M. A., M. D. Lilley, and J. A. Baross, 1993. Methane oxidation in deep-sea hydrothermal plumes of the endeavour segment of the Juan de Fuca Ridge, Deep-Sea Res. Pt. I 40: 1169-1186, doi:http://dx.doi.org/10.1016/0967-0637(93)90132-M.

Eller, G., S. Stubner, and P. Frenzel, 2001. Group-specific 16S rRNA targeted probes for the detection of type I and type II methanotrophs by fluorescence in situ hybridisation, FEMS Microbiol. Lett. 198: 91-97, doi:10.1111/j.1574-6968.2001.tb10624.x.

Etiope, G., and R. W. Klusman, 2002. Geologic emission of methane to the atmosphere, Chemosphere 49: 777-789.

Fischer, P. J. (1977), Natural gas and oil seeps, Santa Barbara Basin, CaliforniaRep., 1-62 pp, State Lands Commission, Sacramento.

Haeckel, M., B. P. Boudreau, and K. Wallmann, 2007. Bubble-induced porewater mixing: A 3-D model for deep porewater irrigation, Geochim. Cosmochim. Acta 71: 5135-5154, doi:http://dx.doi.org/10.1016/j.gca.2007.08.011.

Hanson, R. S., and T. E. Hanson, 1996. Methanotrophic bacteria., Microbiol. Rev. June 1996: 439-471.

Hornafius, J. S., D. Quigley, and B. P. Luyendyk, 1999. The world's most spectacular marine hydrocarbon seeps (Coal Oil Point, Santa Barbara Channel, California): quantification of emissions, J. Geophys. Res. 104: 20703-20711.

Huttunen, J. T., K. M. Lappalainen, E. Saarijärvi, T. Väisänen, and P. J. Martikainen, 2001. A novel sediment gas sampler and a subsurface gas collector used for measurement of the ebullition of methane and carbon dioxide from a eutrophied lake, Science of The Total Environment 266: 153-158, doi:http://dx.doi.org/10.1016/S0048-9697(00)00749-X.

IPCC (2013), Climate Change 2013: The Physical Science Basis. Contribution of Working Group I to the Fifth Assessment Report of the Intergovernmental Panel on Climate Change 1535 pp., Cambridge University Press, Cambridge (UK) and New York (USA).

Jakobs, G., P. Holtermann, C. Berndmeyer, G. Rehder, M. Blumenberg, G. Jost, G. Nausch, and O. Schmale, 2014. Seasonal and spatial methane dynamics in the water column of the central Baltic Sea (Gotland Sea), Continental Shelf Research, doi:10.1016/j.csr.2014.07.005.

Judd, A. G., and M. Hovland (2007), Seabed Fluid Flow: The Impact of Geology, Biology and the Marine Environment, Cambridge University Press.

Kinnaman, F., J. Kimball, L. Busso, D. Birgel, H. Ding, K.-U. Hinrichs, and D. Valentine, 2010. Gas flux and carbonate occurrence at a shallow seep of thermogenic natural gas, Geo-Mar. Lett. 30: 355-365, doi:10.1007/s00367-010-0184-0.

Knittel, K., and A. Boetius, 2009. Anaerobic Oxidation of Methane: Progress with an Unknown Process, Annu. Rev. Microbiol. 63: 311-334.

Knittel, K., T. Losekann, A. Boetius, R. Kort, and R. Amann, 2005. Diversity and distribution of methanotrophic archaea at cold seeps, Appl. Environ. Microbiol. 71: 467-479, doi:10.1128/aem.71.1.467-479.2005.

Leifer, I., 2010. Characteristics and scaling of bubble plumes from marine hydrocarbon seepage in the Coal Oil Point seep field, J. Geophys. Res.-Oceans 115: C11014, doi:10.1029/2009JC005844.

Leifer, I., and J. F. Clark, 2002. Modeling trace gases in hydrocarbon seep bubbles: Application to marine hydrocarbon seeps in the Santa Barbara Channel, Russian Journal of Geology and Geophysics 47: 572-579.

Leifer, I., and D. Culling, 2010. Formation of seep bubble plumes in the Coal Oil Point seep field, Geo-Marine Letters 30: 339-353.

Leifer, I., G. De Leeuw, and L. H. Cohen, 2003. Optical measurements of bubbles: system design and application, J. of Atmos. Ocean Tech. 20: 1317-1332.

Leifer, I., and A. G. Judd, 2002. Oceanic methane layers: The hydrocarbon seep bubble deposition hypothesis, Terra Nova 14: 417-424.

Leifer, I., M. Kamerling, B. P. Luyendyk, and D. Wilson, 2010. Geologic control of natural marine hydrocarbon seep emissions, Coal Oil Point seep field, California, Geo-Mar. Lett. 30: 331-338.

Leifer, I., B. Luyendyk, and K. Broderick, 2006. Tracking an oil slick from multiple natural sources, Coal Oil Point, California, Marine and Petroleum Geology 23: 621-630, doi:http://dx.doi.org/10.1016/j.marpetgeo.2006.05.001.

Leifer, I., and R. K. Patro, 2002. The bubble mechanism for methane transport from the shallow sea bed to the surface: A review and sensitivity study, Continental Shelf Research 22: 2409-2428.

Mau, S., M. B. Heintz, and D. L. Valentine, 2012. Quantification of CH_4 loss and transport in dissolved plumes of the Santa Barbara Channel, California, Cont. Shelf Res. 32: 110-120.

McGinnis, D. F., J. Greinert, Y. Artemov, S. E. Beaubien, and A. Wüest, 2006. Fate of rising methane bubbles in stratified waters: How much methane reaches the atmosphere?, J. Geophys. Res. 111: C09007, doi:10.1029/2005jc003183.

Michaelis, W., et al., 2002. Microbial reefs in the Black Sea fueled by anaerobic oxidation of methane, Science 297: 1013-1015.

Nauhaus, K., M. Albrecht, M. Elvert, A. Boetius, and F. Widdel, 2007. In vitro cell growth of marine archaeal-bacterial consortia during anaerobic oxidation of methane with sulfate, Environ. Microbiol. 9: 187-196.

NOAA 2013. global monitoring division measurement location Maua Loa, http://www.esrl.noaa.gov/gmd/dv/iadv/, edited, Hawaii, USA.

Pape, T., A. Bahr, J. Rethemeyer, J. D. Kessler, H. Sahling, K.-U. Hinrichs, S. A. Klapp, W. S. Reeburgh, and G. Bohrmann, 2010. Molecular and isotopic partitioning of low-molecular-weight hydrocarbons during migration and gas hydrate precipitation in deposits of a high-flux seepage site, Chem. Geol. 269: 350-363, doi:http://dx.doi.org/10.1016/j.chemgeo.2009.10.009.

Peckmann, J., A. Reimer, U. Luth, C. Luth, B. T. Hansen, C. Heinicke, J. Hoefs, and J. Reitner, 2001. Methane-derived carbonates and authigenic pyrite from the northwestern Black Sea, Mar. Geol. 177: 129-150.

Pernthaler, A., J. Pernthaler, and R. Amann, 2002. Fluorescence In Situ Hybridization and Catalyzed Reporter Deposition for the Identification of Marine Bacteria, Appl. Environ. Microbiol. 68: 3094-3101, doi:10.1128/aem.68.6.3094-3101.2002.

Powelson, D. K., and A. L. Mills, 1998. Water saturation and surfactant effects on bacterial transport in sand columns, Soil Science 163: 694-704.

Reeburgh, W. S., 2007. Ocean methane biogeochemistry, Chem. Rev. 107: 486-513.

Rehder, G., R. S. Keir, and E. Suess, 1999. Methane in the northern Atlantic controlled by microbial oxidation and atmospheric history, Geophys. Res. Lett. 26: 587-590.

Sadhal, S. S., and R. E. Johnson, 1983. Stokes flow past bubbles and drops partially coated with thin films. Part 1. Stagnant cap of surfactant film - exact solution, Journal of Fluid Mechanics 126: 237-250.

Schaefer, A., H. Harms, and A. J. B. Zehnder, 1998. Bacterial Accumulation at the Air-Water Interface, Environ. Sci. Technol. 32: 3704-3712.

Schippers, A., L. N. Neretin, J. Kallmeyer, T. G. Ferdelman, B. A. Cragg, R. John Parkes, and B. B. Jorgensen, 2005. Prokaryotic cells of the deep sub-seafloor biosphere identified as living bacteria, Nature 433: 861-864.

Schmale, O., S. E. Beaubien, G. Rehder, J. Greinert, and S. Lombardi, 2010. Gas seepage in the Dnepr paleo-delta area (NW-Black Sea) and its regional impact on the water column methane cycle, J. Marine Syst. 80: 90-100.

Schmale, O., M. Blumenberg, K. Kießlich, G. Jakobs, C. Berndmeyer, M. Labrenz, V. Thiel, and G. Rehder, 2012a. Aerobic methanotrophy within the pelagic redox-zone of the Gotland Deep (central Baltic Sea), Biogeosciences 9: 4969-4977.

Schmale, O., M. Walter, J. Schneider von Deimling, J. Sültenfuß, S. Walker, G. Rehder, and R. Keir, 2012b. Fluid and gas fluxes from the Logatchev hydrothermal vent area, Geochem. Geophys. Geosyst. 13: Q07007.

Schneider von Deimling, J., J. Brockhoff, and J. Greinert, 2007. Flare imaging with multibeam systems: Data processing for bubble detection at seeps, Geochem., Geophys., Geosyst. 8: Q06004, doi:10.1029/2007GC001577.

Schubert, C., E. Durisch-Kaiser, C. P. Holzner, L. Klauser, B. Wehrli, O. Schmale, J. Greinert, D. McGinnis, M. De Batist, and R. Kipfer, 2006. Methanotrophic microbial communities associated with bubble plumes above gas seeps in the Black Sea, Geochem., Geophys., Geosyst. 7: doi: 10.1029/2005GC001049.

Shakhova, N., I. Semiletov, A. Salyuk, V. Yusupov, D. Kosmach, and Ö. Gustafsson, 2010. Extensive Methane Venting to the Atmosphere from Sediments of the East Siberian Arctic Shelf, Science 327: 1246-1250.

Shimeta, J., C. L. Amos, S. E. Beaulieu, and O. M. Ashiru, 2002. Sequential resuspension of protists by accelerating tidal flow: Implications for community structure in the benthic boundary layer, Limnol. Oceanogr. 47: 1152-1164.

Sommer, S., O. Pfannkuche, P. Linke, R. Luff, J. Greinert, M. Drews, S. Gubsch, M. Pieper, M. Poser, and T. Viergutz, 2006. Efficiency of the benthic filter: Biological control of the emission of dissolved methane from sediments containing shallow gas hydrates at Hydrate Ridge, Global Biogeochem. Cy. 20: GB2019, doi:10.1029/2004GB002389.

Stolle, C., K. Nagel, M. Labrenz, xfc, and K. rgens, 2009. Bacterial activity in the sea-surface microlayer: in situ investigations in the Baltic Sea and the influence of sampling devices, Aquat. Microb. Ecol. 58: 67-78.

Tavormina, P. L., U. Ussler III, and V. Orphan, 2008. Planktonic and Sediment-Associated Aerobic Methanotrophs in Two Seep Systems along the North American Margin, Appl. Environ. Microbiol. 74: 3985-3995.

Treude, T., K. Knittel, M. Blumenberg, R. Seifert, and A. Boetius, 2005a. Subsurface microbial methanotrophic mats in the Black Sea, Appl. Environ. Microbiol. 71: 6375-6378.

Treude, T., M. Krüger, A. Boetius, and B. B. Jørgensen, 2005b. Environmental control on anaerobic oxidation of methane in the gassy sediments of Eckernförde Bay (German Baltic), Limnol. Oceanogr. 50: 1771-1786.

Treude, T., V. Orphan, K. Knittel, A. Gieseke, C. H. House, and A. Boetius, 2007. Consumption of methane and CO2 by methanotrophic microbial mats from gas seeps of the anoxic Black Sea, Appl. Environ. Microbiol. 73.7: 2271-2283.

Treude, T., and W. Ziebis, 2010. Methane oxidation in permeable sediments at hydrocarbon seeps in the Santa Barbara Channel, California, Biogeosciences 7: 3095-3108, doi:doi:10.5194/bg-7-3095-2010.

Upstill-Goddard, R., T. Frost, G. R. Henry, M. Franklin, J. C. Murrel, and N. J. P. Owens, 2003. Bacterioneuston control of air-water methane exchange determined with a laboratory gas exchange tank, Global Biogeochem. Cy. 17: 19.11-19.15.

Valentine, D. L., 2011. Emerging topics in marine methane biogeochemistry, Annu. Rev. Marine. Sci. 3: 147-171.

Valentine, D. L., D. C. Blanton, R. W. S., and M. Kastner, 2001. Water column methane oxidation adjacent to an area of active hydrate dissociation, El River Basin, Geochim. Cosmochim. Acta 65: 2633-2640.

Wallace, G. T., and R. A. Duce, 1978. Transport of particulate organic matter by bubbles in marine waters, Limnol. Oceanogr. 23: 1155-1167.

Wan, J., and J. L. Wilson, 1994. Visualization of the role of the gas-water interface on the fate and transport of colloids in porous nedia, Water Resour. Res. 30: 11-23.

Wan, J., J. L. Wilson, and T. L. Kieft, 1994. Influence of the gas-water interface on transport of microorganisms through unsaturated porous madia, Appl. Environ. Microbiol. 60: 509-516.

Westbrook, G. K., et al., 2009. Escape of methane gas from the seabed along the West Spitsbergen continental margin, Geophy. Res. Lett. 36: L15608, doi:10.1029/2009GL039191.

Zhou, J., and K. Mopper, 1998. The role of surface-active carbohydrates in the formation of transparent exopolymer particles by bubble adsorption of seawater Limnol. Oceanogr. 43: 1860-1871.

Figure captions

Figure 1. Map of sonar-derived seepage activity in the Coal Oil Point (COP) seep field. Adapted from (Leifer et al., 2010a). Rostocker Seep (red dot) is at 34°24.230' N; 119°50.428' W.

Figure 2. The sketch shows the concept of the Bubble Transport Mechanism and the technical drawing of the bubble catcher. The bubble catcher is positioned on the seafloor above a gas

vent. Gas bubbles (gray circles) rise within sediment voids, collect microbial cells (red circles), and transport microbial cells from the sediment, through the water, into the bubble catcher. During the "BC vent" experiment (see text) the gas bubble stream was focused by a funnel (1, positioned ca. 2 cm above the seafloor) and transferred into the sample cylinder (3) through the stop-cock (2). The gas bubbles moved further upwards through the sterile-filtered artificial seawater (4) and released the attached surfactants at the gas-water interface within the cylinder. After the gas bubble sampling the stop-cock (2) was closed. The pressure compensation during the recovery of the bubble catcher was controlled by a relief pressure valve (6). Through stop-cock 2 and 5, the bubble catcher sample water was released and the inner part of the sample cylinder was rinsed. During seafloor deployments, three frame legs stabilized the sampling cylinder. The insert shows the set-up of the "BC blank" experiment, where gas bubbles were released from a pressurized nitrogen tank that was situated above the seafloor (7).

Figure 3. (A) Funnel and stop-cock of the bubble catcher during gas bubble sampling in the "BC vent" experiment. (B) Sample cylinder with gas-water interface. The scale bar is 100 mm.

Figure 4. Bubble emission size distribution, Φ, and volume flux, V, as a function of radius, r, and Gaussian fits to emission modes of Φ. Data key on figure. Φ is the number of bubbles (#) that cross an arbitrary horizontal plane per second in each (logarithmically-spaced) r-bin.

Figure 5. (A) Sediment methane (CH_4) concentrations profiles from the Rostocker Seep. (B) Total cell abundance (DAPI, black circles), as well as aerobic methane oxidation bacteria (MOB, red diamonds) and anaerobic methanotrophs (ANME-2, blue triangles) cell abundance (CARD-FISH) in sediment samples.
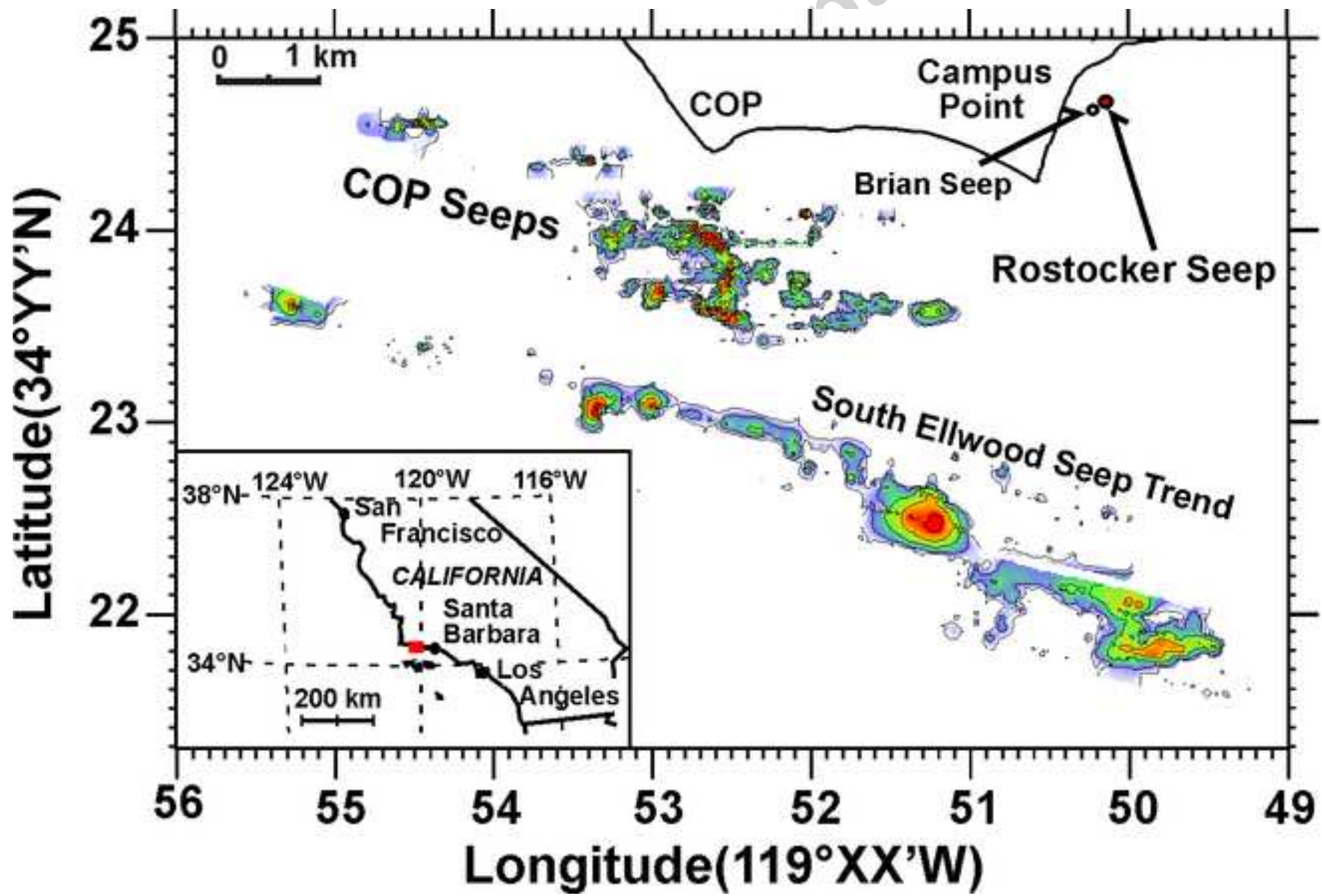
Figure 6. (A) Water column methane (CH$_4$) concentrations at Rostocker Seep. (B) Total cell abundance (DAPI, black circles), as well as aerobic methane oxidizing bacteria (MOB, red diamonds, CARD-FISH) in water column samples. Anaerobic methanotrophs (ANME-2, CARD-FISH) were not detected in any water samples.

Figure 7. Epifluorescence images of MOB and ANME-2 cells visualized by 4', 6-Diamidin-2-phenylindol (DAPI, blue = A, C, E) and Catalyzed Reporter Deposition Fluorescence in Situ Hybridization (CARD-FISH, Alexa 488, green = B, D, F). MOB cells were identified applying CARD-FISH with the combined probes M(α)450, M(γ)84, and M(γ)705. ANME-2 cells were identified using probe ANME 2-538. (A, B) Aggregate of MOB cells obtained from the "BC vent" experiment. (C, D) MOB cells present in 1 cm sediment depth at the seep gas vent. (E, F) ANME-2 aggregate present in 3 cm sediment depth at the seep gas vent. The scale bar is 10 μm.

Highlights

1. A new bentho-pelagic transport mechanism of microorganisms is hypothesized

2. A bubble transport hypothesis was tested using a new gas bubble-collecting device

3. Bubble-mediated transport rate of methanotrophs was quantified at a gas vent

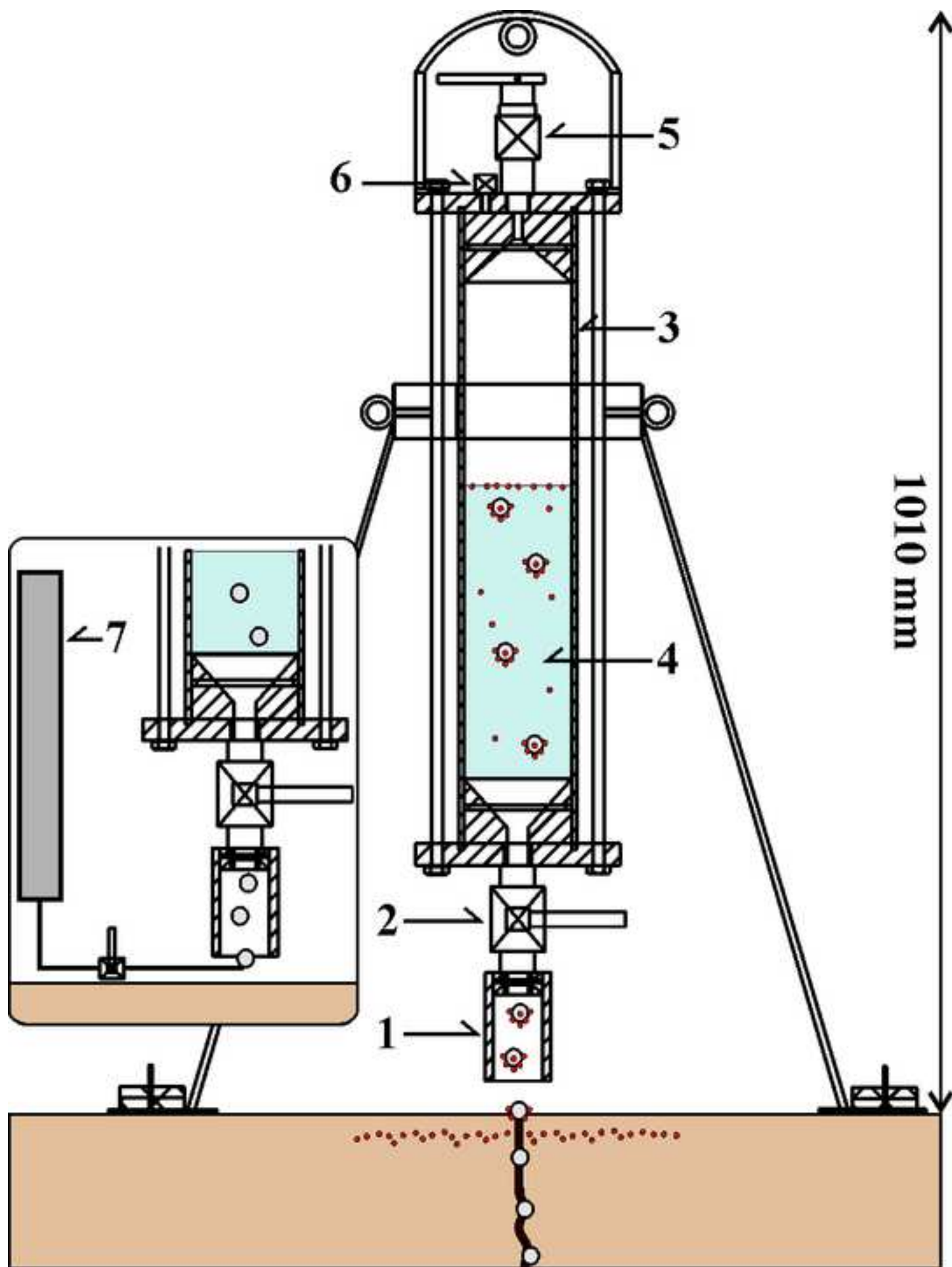4. The Bubble Transport Mechanism may influence the pelagic methane sink
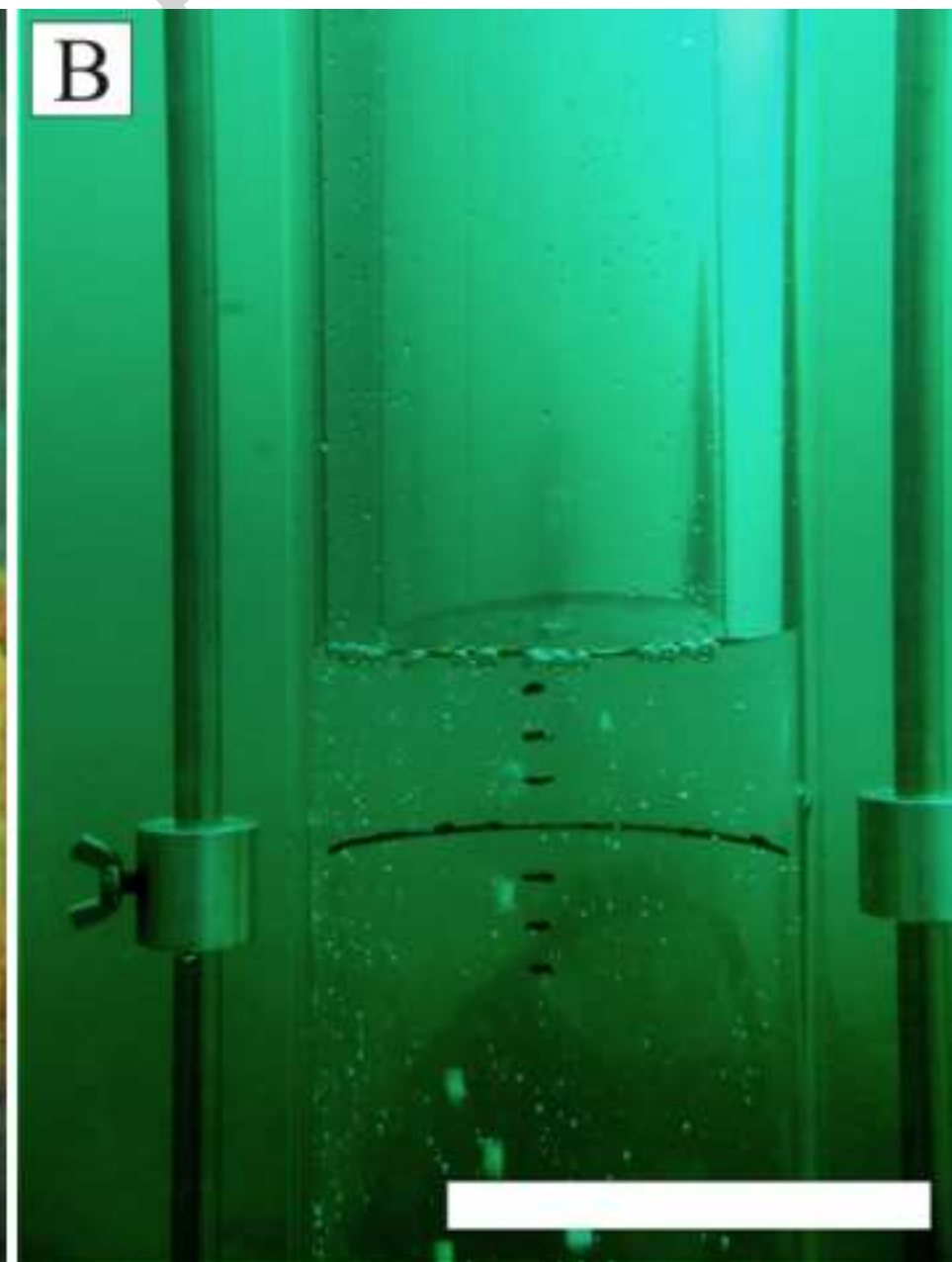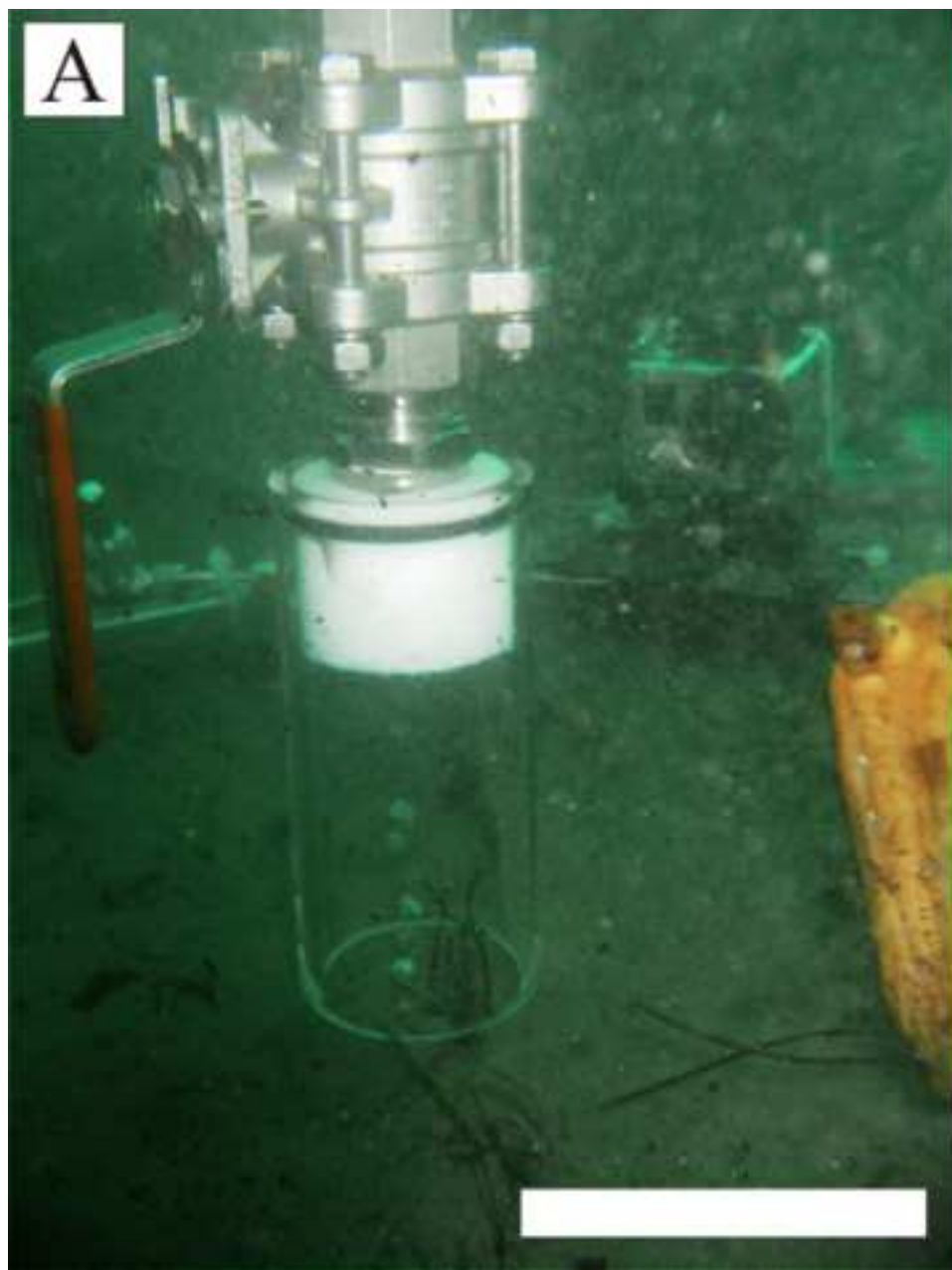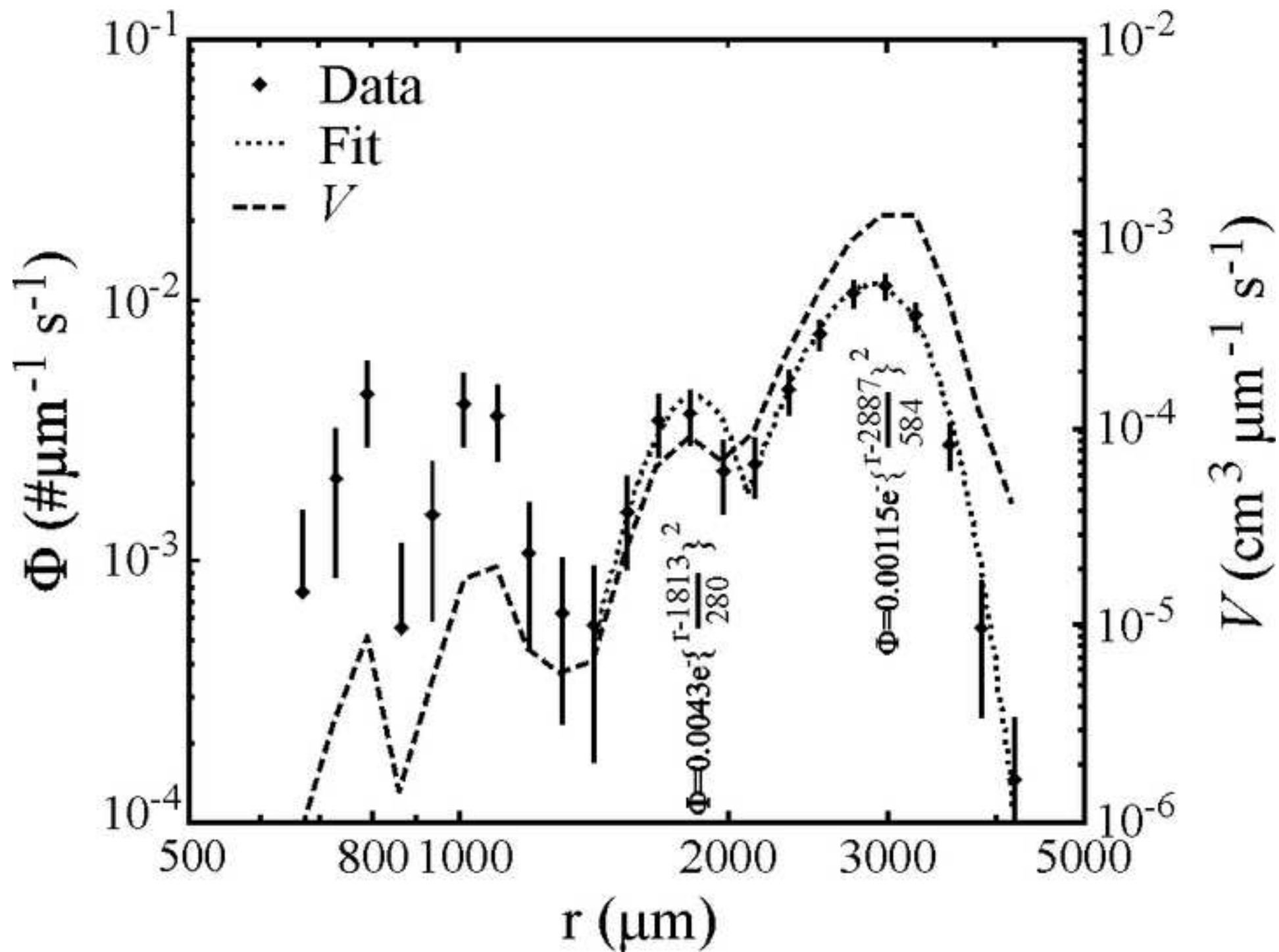
Figure 1

Figure 2

Figure 3

Figure 4

$$\Phi = 0.0043 e^{-\left\{\frac{r-1813}{280}\right\}^2}$$

$$\Phi = 0.00115 e^{-\left\{\frac{r-2887}{584}\right\}^2}$$

Figure 5

Figure 6

Figure 7